

Chance-Constrained Water Pumping to Manage Water and Power Demand Uncertainty in Distribution Networks

This article demonstrates how water pumping in drinking water distribution networks can be treated as a flexible load in the power distribution network.

By Anna Stuhlmacher[©], Student Member IEEE, and Johanna L. Mathieu[©], Senior Member IEEE

ABSTRACT | Water pumping in drinking water distribution networks (WDNs) can be treated as a flexible load in the power distribution network (PDN). In this article, we formulate an optimization problem to minimize the electricity costs associated with pumping subject to WDN and PDN constraints. In practice, both water and power demands are uncertain and pumps should be scheduled to ensure that pump operation does not violate either networks' constraints for nearly all possible uncertainty realizations. To address this problem, we formulate a chance-constrained (CC) optimization problem that simultaneously determines pumping schedules along with the parameters of real-time control policies that can be used to respond to water and power demand forecast errors. We use approximations and relaxations along with the scenario approach for CC programming to reformulate the optimization problem into a convex deterministic problem. We demonstrate the performance of the approach through case studies and also explore the impact of the relaxations, an approach to improve computational tractability, and tradeoffs associated with the way in which we define the cost of real-time control actions. We find

Manuscript received November 3, 2019; revised February 13, 2020 and May 11, 2020; accepted May 19, 2020. Date of publication June 16, 2020; date of current version August 20, 2020. This work was supported in part by a National Science Foundation Graduate Research Fellowship under Grant DGE 1256260 and in part by the National Science Foundation under Grant ECCS-1845093. (Corresponding author: Anna Stuhlmacher.)

The authors are with the Department of Electrical Engineering and Computer Science, University of Michigan, Ann Arbor, MI 48109 USA (e-mail: akstuhl@umich.edu; jlmath@umich.edu).

Digital Object Identifier 10.1109/JPROC.2020.2997520

that optimal scheduling and real-time control of water pumping can effectively manage water and power demand uncertainty, meaning water demand is satisfied and both the WDN and PDN operate within their limits; however, the approach is conservative leading to high reliability at high cost.

KEYWORDS ¹ Chance-constrained (CC) programming; electric power distribution networks (PDNs); water distribution networks (WDNs).

I. INTRODUCTION

There is growing interest in understanding the benefits and drawbacks of optimizing operations across multiple coupled critical infrastructure systems [1]. Potential benefits include increased flexibility, sustainability, and reliability as well as reduced capital and operational costs. However, formulating and solving such an optimization problem may be computationally taxing or intractable due to the system's scale and nonconvexity. A significant body of work has demonstrated the benefits of optimizing multienergy systems, for example, natural gas/grid networks [2] and district heating/grid networks [3]. In the latter, both district heating and electricity could be provided by a combined heat and power plant, which is operated subject to constraints from both the electricity distribution network and the hot water network. Other types of water networks are also strongly coupled with electricity networks. For example, agricultural water pumps can be used within demand response programs to provide economic benefits

0018-9219 © 2020 IEEE. Personal use is permitted, but republication/redistribution requires IEEE permission. See https://www.ieee.org/publications/rights/index.html for more information.

to and improve the reliability of the power system [4]. Drinking water and wastewater treatment plants have also been used for demand response [5]. Using these electricity-consuming water network assets to reduce the cost and/or increase the reliability of power systems in turn reduces the cost of water networks (via cheaper electricity) and improves their reliability (via fewer pumping/treatment outages that results from power outages).

In this article, we explore the coupling between the water distribution network (WDN) and the power distribution network (PDN). Both distribution networks are facing growing challenges. For example, the WDN requires more energy-intensive methods for distributing drinking water due to a shrinking freshwater supply and the PDN is experiencing increasing levels of intermittent, uncertain renewable energy resources such as solar photovoltaics [6]. Additionally, both networks are facing increasing levels of consumer demand. These two networks are intrinsically interdependent: water pumps in the WDN are loads in the PDN and water storage tanks allow for shifting pumping in time. Drinking and waste water networks consume around 4% of the electricity use in the United States, where a majority of that consumption (90%–99%) is used for pumping [7]. Regionally, this percentage can be considerably larger. For example, in California 19% of all energy consumption goes to water-related uses [8]. Despite the WDN's significant energy consumption and the inherent coupling of the WDN and PDN, the WDN is usually treated as an uncontrollable load on the PDN.

Our goal is to develop operational and real-time control strategies that use WDN water pumps and tanks to support PDNs facing uncertainty from distributed energy resources, which leads to uncertainty in net power demand. Specifically, with increased penetrations of solar photovoltaics, PDNs can experience unexpected net demand fluctuations that cause voltage fluctuations, in some cases leading to voltage problems. Flexible loads, like WDN pumps, can be used to mitigate those problems, improving the reliability of the PDN and in turn improving the reliability of the WDN. Most urban WDNs have automated, computerized supervisory control and data acquisition (SCADA) systems, and are capable of fast operational control [7]. For example, Pabi et al. [9] reported the results of a water treatment plant with a SCADA system participating in a demand response program; the plant was able to respond in seconds. We formulate an optimization problem to schedule pumping and tank levels subject to both WDN and PDN constraints and considering uncertainty in both nodal net power demands and the water demands. There are two challenges to solving this problem. First, the networks include nonlinear and nonconvex constraints. The second challenge is how to handle the uncertainty. We address the former by using convex approximations and relaxations, and provide a discussion on how they impact the solution. We address the latter by developing affine real-time control policies to respond to water and power demand forecast errors and formulating the problem as a

chance-constrained (CC) optimization problem that jointly solves for the WDN schedule and control policies' parameters. Since these are critical infrastructure networks, we care more about feasibility than minimizing costs, and chance constraints allow us to achieve constraint satisfaction at high probability levels. However, we also acknowledge that a CC programming formulation has certain limitations and highlight these within this article.

Although related to the problem of optimizing district heating/grid systems (see [3] and [10]–[14]), our problem is different. Unlike problems that optimize the operation of a centralized combined heat and power plant, our problem optimizes resources (pumps and tanks) that may be distributed across the WDN/PDN. Additionally, while the goal of WDNs is to meet water demand, the goal of district heating networks is to meet heat demand; hot water and electricity may also be delivered but that is not the primary goal of these networks. That means optimizing district heating/grid systems requires modeling additional components (e.g., heat exchangers, heat pump units, and combined heat and power plants) and including heat transfer constraints, which we do not consider here. Furthermore, district heating networks are not geographically extensive due to high-investment cost and lossy heat transport [13], while WDNs can be much larger. However, the problems are similar in that both district heating networks and WDNs must manage uncertainty. Mancarella et al. [13] identified the need for more planning and operation research for heating-electricity systems that include uncertainty. There is a similar gap in the literature for WDN-PDN systems.

Our work builds on a significant body of research on the optimal operation of WDNs. In most of the work, the objective is to minimize operational costs or improve water quality. Most articles solve deterministic problems. Solution approaches include the gradient method [15], [16], linear approximations [17], or genetic algorithms [18]. Ghaddar et al. [19] used a Lagrangian decomposition to improve computation time and Fooladivanda and Taylor [20] applied relaxations and utilized distributed optimization to compute the suboptimal operation. Mala-Jetmarova et al. [21] and Ormsbee and Lansey [22] provided a literature review on WDN operational control methodologies. Several articles consider uncertainty when optimizing the WDN's operation [23]-[25] and design [26]-[28]. Most of these approaches use simplified WDN models.

There is also a substantial body of work on the optimal operation of power networks; we refer the reader to [29] for a comprehensive review. There is also work on formulating and solving CC optimization programs for power networks [30], [31] with control policies enabling real-time response to forecast errors [32], [33].

There is growing interest in the integrated optimization of water and power networks. In [34], a water-power flow optimization problem and a distributed solution approach are developed. Li *et al.* [35] applies relaxations and

approximations to the water-power flow problem to provide demand response from agricultural irrigation systems. In [36], the WDN responds to a signal from the PDN to consume surplus energy at times of excess generation. Oikonomou and Parvania [37] used multiple WDNs to provide electricity-consumption flexibility to the power transmission network. In all of these articles, consumer water and power demand are assumed to be known.

To the best of our knowledge, there are no existing approaches to optimize WDN operation subject to both WDN and PDN constraints considering uncertainty, beyond our preliminary work [38], [39]. In [38], we considered only water demand uncertainty while, in [39], we considered only power demand uncertainty. In this article, we consider both, allowing us to formulate the complete problem and gain substantive additional insights into the solutions of real-world problems. Stuhlmacher and Mathieu [38] developed a first version of a balancing control policy that adjusts pump flow rates in real time to compensate water demand forecast error; in this article, we extend the balancing control policy to include actions from tanks. Also, in [38], we formulated the problem as a nonconvex program and applied a heuristic scenario-based approach to solve it, whereas in this article we use convex approximations and relaxations so that we can obtain probabilistic guarantees on the solution generated by the scenario approach [40], though the guarantees apply to the approximate/relaxed problem. Stuhlmacher and Mathieu [39] developed a first version of a corrective control policy that adjusts pump flow rates in real time to respond to voltage violations; in this article, we extend it to improve the computational tractability of our solution approach.

The contributions of this article are: 1) the formulation of an optimal multiperiod WDN operation and control problem subject to WDN and PDN constraints and considering uncertainty in both water and power demand; 2) the development of real-time control policies that adjust pump flow rates in response to water and power demand forecast error; 3) the reformulation of the problem into a convex deterministic problem via convex approximations, convex relaxations, and application of the scenario approach; and 4) case studies on a coupled WDN-PDN with pumps, tanks, PDN unbalance, and significant water and power demand uncertainty. Within the case studies, we explore the impact of the approximations and relaxations, an approach to improve computational tractability, and tradeoffs in the way we define the cost of real-time control actions. Including both the balancing and corrective control policies enables us to analyze their relative importance and impact on the optimal solution.

II. PROBLEM DESCRIPTION

Our goal is to minimize WDN electricity costs over a scheduling horizon by choosing supply pump flow rates and tank net outflows together with the parameters of real-time control policies enabling response to water and power demand forecast errors. First, ignoring uncertainty, we can formulate the deterministic optimization problem as

$$\min_{\mathbf{x}} \sum_{t \in \mathcal{T}} F^{t}(\mathbf{x})$$
s.t. $z_{1}(\mathbf{x}, \boldsymbol{\xi}) = 0$, $v_{1}(\mathbf{x}, \boldsymbol{\xi}) \leq 0$

$$z_{2}(\mathbf{x}, \boldsymbol{\xi}) = 0$$
, $v_{2}(\mathbf{x}, \boldsymbol{\xi}) \leq 0$ (D1)

where ${\bf x}$ are the decision variables including supply pump flow rates and tank net outflows (defined later), and ${\boldsymbol \xi}$ are the network parameters including the forecasted water and power demand (also defined later). The cost in discrete time period $t\in {\mathcal T}$ of duration ΔT is

$$F^{t}(\mathbf{x}) := \sum_{e \in \mathcal{P}} \left(\pi_{e}^{t} \Delta T \sum_{\phi \in \Phi} \left(p_{e,\phi}^{t} \right) \right) \quad \forall \ t \in \mathcal{T}$$
 (1)

where π_e^t is the actual or forecasted price of electricity for pump $e \in \mathcal{P}$ and $p_{e,\phi}^t$ is the power consumption of pump e on PDN phase $\phi \in \Phi = \{a,b,c\}$. Functions $z_1(\mathbf{x},\boldsymbol{\xi})$ and $v_1(\mathbf{x},\boldsymbol{\xi})$ are the PDN's equality and inequality constraints, and $z_2(\mathbf{x},\boldsymbol{\xi})$ and $v_2(\mathbf{x},\boldsymbol{\xi})$ are the WDN's equality and inequality constraints. In general, the problem is nonconvex due to nonlinear and nonconvex WDN and PDN constraints. The formulation assumes the WDN has full knowledge of the PDN. While this may be unrealistic, it is still valuable to solve this problem as it gives us insights into the optimal solution achievable without considering limitations on measurements, communication systems, and information sharing by the PDN.

In this section, we first explain the PDN model that defines $z_1(\mathbf{x}, \boldsymbol{\xi})$ and $v_1(\mathbf{x}, \boldsymbol{\xi})$, and then the WDN model that defines $z_2(\mathbf{x}, \boldsymbol{\xi})$ and $v_2(\mathbf{x}, \boldsymbol{\xi})$. Then, we describe a number of convex approximations and relaxations we use, resulting in a convex deterministic problem. Finally, we describe how we incorporate uncertainty, define the cost of flexibility, and formulate our CC optimization problem.

A. PDN Model

The consumers and pumps are connected to a PDN through a set of buses $k \in \mathcal{K}$. The PDN equality constraints $z_1(\mathbf{x}, \boldsymbol{\xi})$ include the three-phase unbalanced ac power flow equations

$$f^{t}\left(\mathbf{P}_{L}^{t}(\mathbf{p}^{t}), \mathbf{Q}_{L}^{t}(\mathbf{q}^{t}), \mathbf{V}^{t}, \boldsymbol{\theta}^{t}, \boldsymbol{\xi}^{t}\right) = 0 \quad \forall \ t \in \mathcal{T}$$
 (2)

where $P_{\mathbf{L}}^t:=[P_{\mathbf{L},k,\phi}^t]_{k\in\mathcal{K},\phi\in\Phi}$ and $Q_{\mathbf{L}}^t:=[Q_{\mathbf{L},k,\phi}^t]_{k\in\mathcal{K},\phi\in\Phi}$ are vectors of the real and reactive power loads at each bus and phase; $V^t:=[V_{k,\phi}^t]_{k\in\mathcal{K},\phi\in\Phi}$ and $\theta^t:=[\theta_{k,\phi}^t]_{k\in\mathcal{K},\phi\in\Phi}$ are vectors of the voltage magnitudes and angles at each bus and phase; and $p^t:=[p_{e,\phi}^t]_{e\in\mathcal{P},\phi\in\Phi}$ and $q^t:=[q_{e,\phi}^t]_{e\in\mathcal{P},\phi\in\Phi}$ are vectors of the real and reactive pump power consumption for each pump and phase, respectively.

The load at each bus and phase is

$$P_{\mathrm{L},k,\phi}^{t} = \begin{cases} \rho_{k,\phi}^{t} + p_{e,\phi}^{t}, & \text{if pump } e \text{ connected to bus } k \\ \rho_{k,\phi}^{t}, & \text{otherwise} \end{cases}$$
(3)

$$Q_{\mathrm{L},k,\phi}^{t} = \begin{cases} \zeta_{k,\phi}^{t} + q_{e,\phi}^{t}, & \text{if pump } e \text{ connected to bus } k \\ \zeta_{k,\phi}^{t}, & \text{otherwise} \end{cases}$$
 (4)

 $\forall k \in \mathcal{K}, \phi \in \Phi, t \in \mathcal{T}$, where $\rho_{k,\phi}^t$ and $\zeta_{k,\phi}^t$ are network parameters, specifically, the forecasted real and reactive net load, that is, actual load minus distributed generation, for example, from solar photovoltaics, at each bus, phase, and time period. The PDN equality constraints also include

$$\theta_{0,a}^t = 0^{\circ}, \quad \theta_{0,b}^t = -120^{\circ}, \quad \theta_{0,c}^t = 120^{\circ} \quad \forall \ t \in \mathcal{T}$$
 (5)

$$V_{0,a}^t = V_{0,b}^t = V_{0,c}^t = 1 \text{ pu} \quad \forall \ t \in \mathcal{T}$$
 (6)

which specify that the substation (i.e., bus 0, without loss of generality) has a fixed and balanced voltage.

The PDN inequality constraints $v_1(\mathbf{x}, \boldsymbol{\xi}) \leq 0$ include limits on the bus voltages' magnitudes

$$V_k^{\min} \le V_{k,\phi}^t \le V_k^{\max} \quad \forall \ k \in \mathcal{K}, \ \phi \in \Phi, \ t \in \mathcal{T}$$

where V_k^{\min} and V_k^{\max} are the lower and upper voltage magnitude limits at bus k. They can also include limits on the apparent power flows along lines $l \in \mathcal{L}$

$$(P_{l,\phi}^t)^2 + (Q_{l,\phi}^t)^2 \le (S_{l,\phi}^{\text{max}})^2 \quad \forall l \in \mathcal{L}, \phi \in \Phi, \ t \in \mathcal{T}$$
 (8)

where $S_{l,\phi}^{\max}$ is the apparent power flow limit for line l and phase ϕ .

We do not model existing voltage regulating equipment (tap changing transformers, switched capacitors, etc.) as it would introduce binary variables, making the problem much harder to solve. Moreover, this allows us to explore the impact of WDN actions alone on PDN voltage levels. Future work will explore how best to model this equipment in our formulation and how this equipment and WDNs can work together to regulate voltages in the most cost-effective manner.

B. WDN Model

We assume supply pump ON/OFF statuses are determined in advance of the scheduling horizon. We also assume pipe water flows do not change direction during the scheduling horizon. These assumptions are commonly used in the literature (see [20], [34], [36], and [37]), to eliminate the need for binary variables. Consequently, we can formulate the WDN as a directed graph $(\mathcal{N}, \mathcal{E})$ composed of a set of nodes \mathcal{N} and a set of edges \mathcal{E} . Nodes can be categorized as junctions $j \in \mathcal{J}$, reservoirs $j \in \mathcal{R}$, or elevated storage tanks $j \in \mathcal{S}$, that is, $\mathcal{N} = \mathcal{J} \cup \mathcal{R} \cup \mathcal{S}$. In this article, the main distinction between tanks and

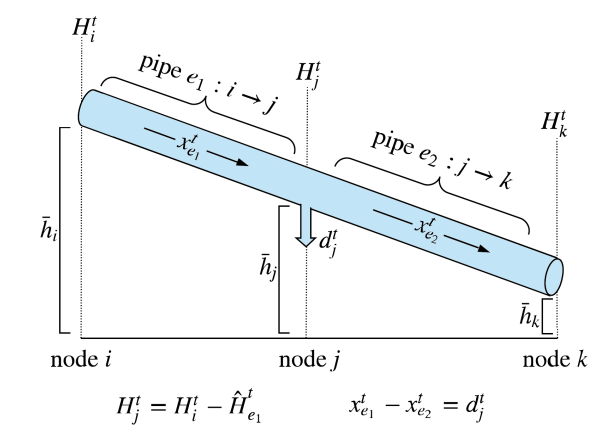


Fig. 1. WDN visualization including elevation and hydraulic head with respect to an elevation reference, flow rate, and head loss. Example equations of conservation of hydraulic head (15) and conservation of water (11) are included.

reservoirs is that tanks allow bidirectional flow whereas reservoirs model the water supply source (i.e., treatment plant clearwells). Water is pumped into elevated storage tanks (e.g., during periods of low demand) so that the tanks can release pressurized water using gravity at a later time period (e.g., during periods of high demand). Edges are pipes connecting the nodes; they can contain a supply pump $e \in \mathcal{P}$ or a pressure reducing valve $e \in \mathcal{V}$, that is, $(\mathcal{P} \cup \mathcal{V}) \subseteq \mathcal{N}$. The WDN can be described by its hydraulic head H_j^t at node j and the volumetric flow rate x_e^t through pipe e. Fig. 1 shows the relationships between elevation, hydraulic head, flow rate, demand, and head loss along two pipe segments.

1) Nodes, \mathcal{N} : The hydraulic head H_j^t at node j is composed of the elevation \bar{h}_j and the pressure head. The WDN nodal constraints are

$$h_j^{\min} + \bar{h}_j \le H_j^t \le h_j^{\max} + \bar{h}_j \quad \forall \ j \in \mathcal{N}, \ t \in \mathcal{T}$$
 (9)

$$H_j^t = \bar{h}_j \quad \forall \ j \in \mathcal{R}, \ t \in \mathcal{T}$$
 (10)

$$\sum_{e \in \mathcal{E}} a_{je} x_e^t = d_j^t \quad \forall j \in \mathcal{J}, \ t \in \mathcal{T}$$
(11)

$$H_{j,\text{out}}^t = H_{j,\text{out}}^{t-1} + \frac{\Delta T}{\gamma_j} \sum_{e \in \mathcal{E}} a_{je} x_e^t \quad \forall \ j \in \mathcal{S}, \ t \in \mathcal{T}$$
 (12)

$$h_j^{\min} + \bar{h}_j \le H_{j,\text{out}}^t \le h_j^{\max} + \bar{h}_j \quad \forall j \in \mathcal{S}, \ t \in \mathcal{T}$$
 (13)

where h_j^{\min} and h_j^{\max} are the lower and upper pressure head limits at node j. For tanks, these are set to the minimum and maximum tank levels. Parameter d_j^t is the forecasted water demand at junction j, γ_j is the cross-sectional area of tank j, and $a_{je} \in \{0,1,-1\}$ is an element in the node-edge incidence matrix which describes the connection of edges and nodes in the network. In (9), the hydraulic head at each node is limited. We treat reservoirs $\mathcal R$ as infinite sources with fixed pressure heads. Consequently in (10), we set the hydraulic head equal to elevation without loss

of generality. For junctions \mathcal{J} , we ensure that the conservation of water is satisfied. Therefore, in (11), the sum of water entering and exiting a junction must equal the consumer water demand d_i^t . We model tanks S with separate inflow and outflow pipes, where the inlet is at the top of the tank and the outlet is at the bottom [41]. The inlet is treated as a junction, where its head H_i^t is computed the same way as any junction (i.e., the upstream hydraulic head minus the head loss through the connecting pipe, described below). The outlet tank hydraulic head $H_{i,\text{out}}^t$ is a function of the previous period's outlet tank hydraulic head and the tank net inflow, as shown in (12). Equation (13) limits the outlet head by the physical volume of the tank. Since we do not want to simply deplete the tank over the scheduling horizon, we constrain the final outlet tank hydraulic head to be greater than or equal to the initial outlet tank hydraulic head

$$H_{j,\text{out}}^{t=|\mathcal{T}|} \ge H_{j,\text{out}}^{t=0}. \tag{14}$$

2) Edges, \mathcal{E} : We denote the frictional head loss along pipe e as $\hat{H}_e^t = -\sum_{j\in\mathcal{N}} a_{je}H_j^t$. The head loss equation for each pipe is dependent on whether it contains a pump or valve

$$\hat{H}_{e}^{t} = \begin{cases} u_{e}(x_{e}^{t}) & \forall e \in \mathcal{P}, \\ L_{e}^{t} & \forall e \in \mathcal{V}, \\ k_{e} \cdot (x_{e}^{t})^{n} & \forall e \in \mathcal{E} \setminus (\mathcal{P} \cup \mathcal{V}), \end{cases}$$
(15a)

 $\forall t \in \mathcal{T}. \text{ The first case corresponds to pipes containing fixed speed pumps, where pump e's hydraulic function u_e is dependent on its flow rate x_e^t. It is usually approximated with a quadratic function. The second case corresponds to pumps containing pressure reducing valves, where the valve head loss $L_e^t \geq 0$ is a decision variable. The third case corresponds to pipes without a pump or valve, where k_e is the resistance coefficient for pipe e and n is the exponent.$

Additionally, the pump flow rates are limited

$$x_e^{\min} \le x_e^t \le x_e^{\max} \quad \forall e \in \mathcal{P}, \ t \in \mathcal{T}$$
 (16)

where $x_e^{\min} > 0$ and x_e^{\max} are the lower and upper flow rate limits for pump e. The power consumption of pump e is a function of its head gain $-\hat{H}_e^t$ and flow rate

$$p_{e,\phi}^t = -\beta_{\phi} \hat{H}_e^t x_e^t \quad \forall \ e \in \mathcal{P}, \ \phi \in \Phi, \ t \in \mathcal{T}$$
 (17)

where β_{ϕ} is a constant with units of kW/CMH \cdot m that both converts $\hat{H}_e^t x_e^t$ to units of power and assigns a portion of the pump power consumption to each phase ϕ , for example, one-third to each phase if the load is balanced.

The WDN equality constraints are collected to form $z_2(\mathbf{x}, \boldsymbol{\xi}) = 0$ and the inequality constraints are collected

to form $v_2(\mathbf{x}, \boldsymbol{\xi}) \leq 0$. The water decision variables are $\boldsymbol{x} := [x_e^t]_{e \in \mathcal{E}, t \in \mathcal{T}}, \ \boldsymbol{H} := [H_j^t]_{j \in \mathcal{N}, t \in \mathcal{T}}, \ \boldsymbol{H}_{\text{out}} := [H_{j, \text{out}}^t]_{j \in \mathcal{S}, t \in \mathcal{T}}, \text{ and } \boldsymbol{L} := [L_e^t]_{e \in \mathcal{V}, t \in \mathcal{T}}.$

C. Deterministic Problem: Nonconvex Formulation

Using the constraints defined in Sections II-A and II-B, the full deterministic problem is given as

$$\begin{aligned} & \min_{\mathbf{x}_1} \sum_{t \in \mathcal{T}} F^t(\mathbf{x}_1) \\ & \text{s.t. } (2) - (8) \\ & (9) - (17) \end{aligned} \tag{D2}$$

where the decision variables are $\mathbf{x}_1 = \{x, H, H_{\text{out}}, L, P_L, Q_L, V, \theta, p, q\}$. The problem is nonconvex.

D. Approximations and Relaxations

Since nonconvex problems can be difficult to solve, we use convex approximations and relaxations to convexify our formulation. For the PDN, we use a linearized three-phase unbalanced power flow model for radial networks; however, our approach can easily be extended to other convex PDN formulations, such as [42] and [43], where [43] approximates system losses. The formulation neglects the losses and assumes that the voltage unbalance at each bus is small [44]

$$Y_k^t = Y_n^t - M_{kn} P_n^t - N_{kn} Q_n^t \quad \forall \ k \in \mathcal{K}, \ t \in \mathcal{T} \quad (18)$$

$$\mathbf{P}_{k}^{t} = \mathbf{P}_{L,k}^{t} + \sum_{n \in \mathcal{I}_{k}} \mathbf{P}_{n}^{t} \quad \forall \ k \in \mathcal{K}, \ t \in \mathcal{T}$$

$$(19)$$

$$\boldsymbol{Q}_{k}^{t} = \boldsymbol{Q}_{L,k}^{t} + \sum_{n \in \mathcal{I}_{k}} \boldsymbol{Q}_{n}^{t} \quad \forall \ k \in \mathcal{K}, \ t \in \mathcal{T}$$
 (20)

where $\boldsymbol{Y}_k^t \in \mathbb{R}^{3 \times 1}$ contains the three-phase voltage magnitudes squared at bus k and time t, that is, $\boldsymbol{Y}_{k,\phi}^t = (V_{k,\phi}^t)^2$; $\boldsymbol{P}_k^t \in \mathbb{R}^{3 \times 1}$ and $\boldsymbol{Q}_k^t \in \mathbb{R}^{3 \times 1}$ contain the three-phase real and reactive power flows entering bus k at time t; and parameter matrices \boldsymbol{M}_{kn} and \boldsymbol{N}_{kn} are formed from the line impedances. The set \mathcal{I}_k contains all buses that are connected directly downstream of bus k.

For the WDN, the head loss in pipes without pumps or valves (15c), the pump hydraulic function (15a), and the pump power consumption (17) are nonconvex. Head loss is usually modeled with the Darcy–Weisbach or Hazen–Williams formulas (see [45] for details). Both are nonconvex. Using the approach from [35], we relax the Darcy–Weisbach formula, in which n=2, by replacing (15c) with its convex hull

$$\hat{H}_{e}^{t} \ge k_{e} \cdot (x_{e}^{t})^{2} \quad \forall e \in \mathcal{E} \setminus (\mathcal{P} \cup \mathcal{V}), \ t \in \mathcal{T}$$
 (21a)

$$\hat{H}_e^t \le b_e^0 + b_e^1 x_e^t \quad \forall e \in \mathcal{E} \setminus (\mathcal{P} \cup \mathcal{V}), \ t \in \mathcal{T}$$
 (21b)

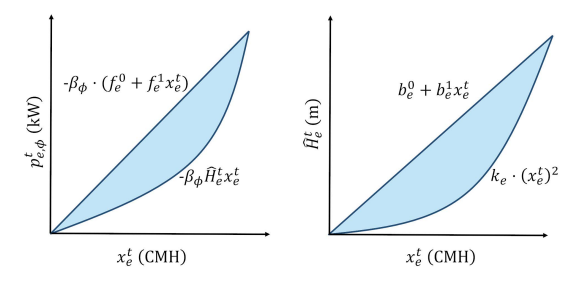


Fig. 2. Convex hull for the pump power consumption (left) and pipe head loss (right).

where b_e^0 and b_e^1 are parameters that provide the upper bound for the convex hull. In Fig. 2 (right), we illustrate the convex hull of the pipe head loss.

As mentioned, the pump hydraulic function (15a) is usually approximated with a quadratic function; however, the coefficient in front of the quadratic term is usually small and negative [45]. Therefore, like [35], we neglect the quadratic term since its contribution is small compared to the linear term and approximate the pump hydraulic function as

$$\hat{H}_e^t = -\left(m_e^0 + m_e^1 \ x_e^t\right) \quad \forall e \in \mathcal{P}, \quad t \in \mathcal{T}$$
 (22)

where m_e^0 and m_e^1 are parameters.

The pump power consumption is a quadratic function of the flow rate x_e^t . Since it is included in the linearized power flow equations, it makes them nonconvex. Again, using the approach from [35], we replace (17) with its convex hull

$$p_{e,\phi}^{t} \geq -\beta_{\phi} \hat{H}_{e}^{t} x_{e}^{t} \quad \forall e \in \mathcal{P}, \phi \in \Phi, \ t \in \mathcal{T}$$

$$p_{e,\phi}^{t} \leq -\beta_{\phi} \cdot \left(f_{e}^{0} + f_{e}^{1} x_{e}^{t} \right) \quad \forall e \in \mathcal{P}, \phi \in \Phi, \ t \in \mathcal{T}$$
(23a)

where f_e^0 and f_e^1 are parameters that provide the upper bound for the convex hull. In Fig. 2 (left), we illustrate the convex hull for the pump power consumption. When pumping costs are minimized subject to the pump power consumption convex hull, the solution will lie on the lower edge of the hull, that is, the original constraint.

E. Deterministic Problem: Convex Formulation

Assuming the PDN experiences voltage problems before apparent power flows violate line limits, which is often the case in radial distribution networks, we neglect the line flow limits (8). Then, using the relaxations and approximations from Section II-D, we can formulate the deterministic problem as a convex program

$$\min_{\mathbf{x}_2} \sum_{t \in \mathcal{T}} F^t(\mathbf{x}_2)
\text{s.t. } (3) - (4), (7), (9) - (14)
(15b), (16), (18) - (23b)$$
(D3)

where the decision variables are $\mathbf{x}_2 = \{x, H, H_{\text{out}}, L, P, Q, Y, p, q\}$.

F. Incorporating Uncertainty

Next, we consider water and power demand uncertainty. We denote the water demand forecast error at junction j as \widetilde{d}_j^t and the power demand forecast error at bus k, phase ϕ as $\widetilde{\rho}_{k,\phi}^t$. We develop control policies to adjust the supply pump flow rates and the tank net outflows from their scheduled operation in real time to balance the mismatch in water supply and demand resulting from water demand forecast error and to correct voltage constraint deviations resulting from power demand forecast error. Note that we do not apply control policies to booster pumps that increase pressure head.

The balancing control policy adjusts pumping and tank levels to compensate for water demand forecast error. We also refer to it as the water control policy. We assume the pumps receive a measurement of the total water demand forecast error and change their flow rates from their schedule by $\widetilde{x}_{\mathbf{w},e}^t$ as a function of the total error $\sum_{j\in\mathcal{J}}\widetilde{d}_j^t$

$$\widetilde{x}_{\mathbf{w},e}^t = c_{\mathbf{w},e}^t \sum_{j \in \mathcal{I}} \widetilde{d}_j^t \quad \forall \ e \in \mathcal{P}, \quad t \in \mathcal{T}$$
 (24)

where $\tilde{x}_{w,e}^t$ is a random variable and $c_{w,e}^t$ is a scalar water control policy parameter associated with pump e and a decision variable in our optimization problem. The tanks are passive and adjust their net outflow by

$$\sum_{e \in \mathcal{E}} -a_{je} \widetilde{x}_{\mathbf{W},e}^t = c_{\mathbf{W},j}^t \sum_{i \in \mathcal{I}} \widetilde{d}_i^t \quad \forall \ j \in \mathcal{S}, \ t \in \mathcal{T}$$
 (25)

to compensate any water demand and supply mismatch, where $c_{\mathrm{w},j}^t$ is a scalar water control policy parameter associated with tank j and a decision variable in our optimization problem. Note that on the right side of the equation we use subscript i rather than j to sum over the water demand forecast errors at all junctions since subscript j is used elsewhere in the equation. To ensure that the water supply equals the water demand we set

$$\sum_{e \in \mathcal{P}} c_{\mathbf{W},e}^t + \sum_{j \in \mathcal{S}} c_{\mathbf{W},j}^t = 1 \quad \forall \ t \in \mathcal{T}.$$
 (26)

Our preliminary work [38] introduced a first version of this control policy, but it did not consider storage tanks or multiple time periods.

The corrective control policy adjusts pumping and tank levels to compensate power demand forecast error when there is a voltage constraint violation. We also refer to it as the power control policy. We assume that pumps receive notice of voltage constraint violations along with measurements of the power demand forecast error for each

bus and phase of the PDN. When violations occur, they change their flow rates from their schedule by $\widetilde{x}_{p,e}^t$ as a function of the error vector $\widetilde{\rho}^t := [\widetilde{\rho}_{k,\phi}^t]_{k \in \mathcal{K}, \phi \in \Phi}$

$$\widetilde{x}_{p,e}^t = C_{p,e}^t \widetilde{\rho}^t \quad \forall e \in \mathcal{P}, \ t \in \mathcal{T}$$
 (27)

where $\widetilde{x}_{\mathrm{p},e}^t$ is a random variable and $C_{\mathrm{p},e}^t$ is a power control policy parameter row vector that relates the power demand deviations at load bus k and phase ϕ to a change in pump e's flow rate. The latter is a decision variable in our optimization problem. Note that (27) does not explicitly control tank levels (recall that tanks do not consume power so they have no direct impact on voltages); however, tanks still compensate for deviations between water supply and demand.

Our preliminary work [39] introduced (27) and found that solving for power control policy parameters corresponding to every load bus and phase was computationally cumbersome. Therefore, in Section III-D, we explore the impact of aggregating forecast errors over phases/buses, which reduces the number of decision variables and therefore the size of the optimization problem. Stuhlmacher and Mathieu [39] also explored use of the power control policy for all power demand forecast errors versus only when needed to correct a voltage constraint violation. While always applying the power control policy would result in unnecessary control actions, it would also eliminate the need for real-time notice of voltage constraint violations. Moreover, modeling the usage/nonusage of the power control policy in the optimization formulation requires introduction of binary variables, which significantly increases computation time [39]. It is also possible to formulate the optimization problem assuming that the power control policy is used for all power demand forecast errors, but only apply it when needed. However, this may result in a suboptimal policy. In this article, we formulate the optimization problem assuming the power control policy is used for all power demand forecast errors and also apply it in this way.

For notational simplicity, we define the water control policy parameter column vector, which includes all pump and tank control policy parameters, as $c_{\rm w}^t:=\langle [c_{{\rm w},e}^t]_{e\in\mathcal{P}},[c_{{\rm w},j}^t]_{j\in\mathcal{S}}\rangle$, where we use angle brackets to vertically stack column vectors. We also define the power control policy matrix $C_{\rm p}^t=[C_{{\rm p},e}^t]_{e\in\mathcal{P}}$, which includes all pumps. Note that the control policy parameters may vary over the scheduling horizon. Both control policies contribute to the total change in pump flow rate

$$\widetilde{x}_{e}^{t} = \widetilde{x}_{\mathbf{w},e}^{t} + \widetilde{x}_{\mathbf{p},e}^{t} \quad \forall \ e \in \mathcal{P}, \ t \in \mathcal{T}.$$
 (28)

G. Flexibility Costs

Using pumps to respond to forecast errors in real time would incur some cost, that is, more frequent changes in output, larger changes in output, and/or faster changes

in output would lead to more wear and tear on WDN components, such as pumps and valves. We refer to this cost as flexibility cost. However, it is not clear how best to formulate that cost and so we explore several options. We define the objective function of the CC optimization problem as $\sum_{t\in\mathcal{T}} \left(F^t(\mathbf{x}_2) + g_{\mathbf{w}}^t G_{\mathbf{w}}^t + g_{\mathbf{p}}^t G_{\mathbf{p}}^t\right)$, where $g_{\mathbf{w}}^t G_{\mathbf{w}}^t$ and $g_{\mathbf{p}}^t G_{\mathbf{p}}^t$ are flexibility cost functions associated with the water and power control policies, respectively, and $g_{\mathbf{w}}^t$ and $g_{\mathbf{p}}^t$ are weighting coefficients. The dimensions of $g_{\mathbf{w}}^t$ and $g_{\mathbf{p}}^t$ are chosen such that the terms $g_{\mathbf{w}}^t G_{\mathbf{w}}^t$ and $g_{\mathbf{p}}^t G_{\mathbf{p}}^t$ are scalars. Three options for defining the flexibility cost follow.

1) Option 1: The flexibility costs are a function of the squared norms of the water and power control policy parameters

$$G_{\mathbf{W},1}^t := ||c_{\mathbf{W}}^t||_2^2 \tag{29}$$

$$G_{p,1}^t := ||C_p^t||_F^2.$$
 (30)

Specifically, we use the squared Euclidean norm of the water control policy parameter vector and the squared Frobenius norm of the power control policy parameter matrix. Therefore, $G_{\mathrm{w},1}^t$ and $G_{\mathrm{p},1}^t$ are scalars. Option 1 penalizes all parameters within the control policy to prevent excessive control actions. For the water control policy, this formulation spreads the control actions amongst the pumps/tanks rather than using only a small subset of pumps/tanks to compensate water demand deviations. For the power control policy, the system is underdetermined, that is, different choices of power control parameters can achieve the same control action given the same power demand forecast error. This formulation chooses the set of parameters that minimizes their squared norm.

2) Option 2: The flexibility costs are a function of the range of pump flow rate adjustments

$$G_{\mathbf{w},2}^t := \langle \mathbf{W}_{\mathbf{up},\mathbf{w}}^t, \mathbf{W}_{\mathbf{dn},\mathbf{w}}^t \rangle \tag{31}$$

$$G_{p,2}^t := \langle \boldsymbol{W}_{up,p}^t, \boldsymbol{W}_{dn,p}^t \rangle \tag{32}$$

where column vectors $\boldsymbol{W}_{\text{up,w}}^t, \boldsymbol{W}_{\text{dn,w}}^t \in \mathbb{R}_+^{|\mathcal{P} \cup \mathcal{S}| \times 1}$ define the flexibility band around the scheduled flow rate for water control policy actions and $\boldsymbol{W}_{\text{up,p}}^t, \boldsymbol{W}_{\text{dn,p}}^t \in \mathbb{R}_+^{|\mathcal{P}| \times 1}$ define the flexibility band for power control policy actions. Specifically, $\boldsymbol{W}_{\text{up,w}}^t, \boldsymbol{W}_{\text{dn,w}}^t, \boldsymbol{W}_{\text{up,p}}^t$, and $\boldsymbol{W}_{\text{dn,p}}^t$ are decision variables related to the control policies through the following element-wise inequalities:

$$-\boldsymbol{W}_{\text{dn,w}}^{t} \leq \mathbf{c}_{w}^{t} \sum_{i \in \mathcal{I}} \widetilde{d}_{j}^{t} \leq \boldsymbol{W}_{\text{up,w}}^{t} \quad \forall t \in \mathcal{T}$$
 (33)

$$-\boldsymbol{W}_{\text{dn,p}}^{t} \leq \boldsymbol{C}_{p}^{t} \tilde{\boldsymbol{\rho}}^{t} \leq \boldsymbol{W}_{\text{up,p}}^{t} \quad \forall \, t \in \mathcal{T}. \tag{34}$$

In contrast to Option 1, Option 2 considers the largest flow rate changes over all of the scenarios instead of penalizing the control policy parameters, which may be more reasonable if pump wear-and-tear is related to the magnitude of fast changes in flow rate.

3) Option 3: The flexibility costs are a function of the range of pump power deviations, which is similar to specifying reserve capacities in electric power systems

$$G_{\text{w.3}}^t := \langle \boldsymbol{R}_{\text{up.w}}^t, \boldsymbol{R}_{\text{dn w}}^t \rangle \tag{35}$$

$$G_{p,3}^t := \langle \boldsymbol{R}_{\text{up,p}}^t, \boldsymbol{R}_{\text{dn,p}}^t \rangle \tag{36}$$

where column vectors $\boldsymbol{R}_{\text{up,w}}^t, \boldsymbol{R}_{\text{dn,w}}^t \in \mathbb{R}_+^{|\mathcal{P}| \times 1}$ define the flexibility band around the scheduled pump power consumption due to water control policy actions and $\boldsymbol{R}_{\text{up,p}}^t, \boldsymbol{R}_{\text{dn,p}}^t \in \mathbb{R}_+^{|\mathcal{P}| \times 1}$ define the flexibility band for power control policy actions. While we could specify these values per phase, we make the realistic assumption that pumps are balanced three-phase motors and power deviations are identical in each phase. Therefore, $\boldsymbol{R}_{\text{up,w}}^t, \boldsymbol{R}_{\text{dn,w}}^t, \boldsymbol{R}_{\text{up,p}}^t$, and $\boldsymbol{R}_{\text{dn,p}}^t$ are identical for each phase, and so we do not specify the phase. Since the pump power consumption curve (17) is monotonically increasing, the largest pump power deviations occur with the largest flow rate adjustments. Therefore, decision variables $\boldsymbol{R}_{\text{up,w}}^t, \boldsymbol{R}_{\text{dn,w}}^t, \boldsymbol{R}_{\text{up,p}}^t$, and $\boldsymbol{R}_{\text{dn,p}}^t$ are directly related to $\boldsymbol{W}_{\text{up,w}}^t, \boldsymbol{W}_{\text{dn,w}}^t, \boldsymbol{W}_{\text{up,p}}^t$, and $\boldsymbol{W}_{\text{dn,p}}^t$, that is

$$R_{\mathsf{dn},\mathsf{w},e}^t = p_e^t - \hat{p}_e(x_e^t - W_{\mathsf{dn},\mathsf{w},e}^t) \quad \forall e \in \mathcal{P}, \ t \in \mathcal{T}$$
 (37)

$$R_{\mathrm{dn,p,e}}^t = p_e^t - \hat{p}_e^t (x_e^t - W_{\mathrm{dn,p,e}}^t) \quad \forall e \in \mathcal{P}, \ t \in \mathcal{T}$$
 (38)

$$R_{\text{up,w},e}^t = \hat{p}_e^t(x_e^t + W_{\text{up,w},e}^t) - p_e^t \quad \forall e \in \mathcal{P}, \ t \in \mathcal{T}$$
 (39)

$$R_{\text{up,p,e}}^t = \hat{p}_e^t(x_e^t + W_{\text{up,p,e}}^t) - p_e^t \quad \forall e \in \mathcal{P}, \ t \in \mathcal{T}$$
 (40)

where the function $\hat{p}_e(x_e^t)$ returns the power consumption of pump e for the flow rate x_e^t . Again, since p_e^t and power deviations are identical in each phase, we do not specify the phase. In contrast to Option 2, there is a nonlinear mapping between the pump adjustments and the flexibility cost, and so using this cost option makes the problem more difficult to solve. Specifically, Option 3 requires (33), (34), and (37)–(40); however, the latter are nonconvex. We replace them with their convex hulls as in Section II-B; however, $R_{\rm dn,p}^t$ and $R_{\rm dn,w}^t$ will be inexact, leading to a reduced downward flexibility band.

We discuss the tradeoffs associated with these options in Section III-E.

H. CC Optimization

To formulate the full CC optimization problem, we first write the stochastic counterparts of the deterministic equality constraints (3), (4), (10)–(12), (15b), (18)–(20), and (22), and inequality constraints (7), (9), (13), (14), (16), (21a), (21b), (23a), and (23b) replacing $\rho_{k,\phi}^t$ with $\rho_{k,\phi}^t + \tilde{\rho}_{k,\phi}^t$ and d_j^t with $d_j^t + \tilde{d}_j^t$. For flexibility cost Option 1, the full set of stochastic constraints comprise

these constraints along with (24), (25), (27), and (28). Options 2 and 3 require additional constraints defined in Section II-G. Eliminating the stochastic equality constraints through substitutions into the stochastic inequality constraints, the stochastic inequality constraints can be put into the form $f(\mathbf{x}_2, \mathbf{c}_w, \mathbf{C}_p, \widetilde{d}, \widetilde{\rho}) \leq 0$ and then transformed into a chance constraint

$$\mathbb{P}(f(\mathbf{x}_2, \mathbf{c}_{\mathsf{w}}, \mathbf{C}_{\mathsf{p}}, \widetilde{d}, \widetilde{\boldsymbol{\rho}}) \le 0) \ge 1 - \epsilon \tag{41}$$

where the constraints should be satisfied jointly for a probability level of at least $1-\epsilon$, where ϵ is the violation level. WDN constraints within the chance constraint are the hydraulic head limits and pump flow rate limits. Because tanks are passive, tanks act to maintain water balance when pump flow rate limits are encountered. PDN constraints within the chance constraint correspond to the voltage limits. Therefore, the chance constraint limits the probability of a hydraulic head, pump flow rate, or voltage violation. Finally, we can write the CC optimization problem. For example, for flexibility cost Option 1, the problem is

$$\begin{split} \min_{\mathbf{x}_{2},\mathbf{c}_{\mathbf{w}},\mathbf{C}_{\mathbf{p}}} & \sum_{t \in \mathcal{T}} \left(F^{t}(\mathbf{x}_{2}) + g^{t}_{\mathbf{w}} J^{t}_{\mathbf{w}} + g^{t}_{\mathbf{p}} J^{t}_{\mathbf{p}} \right) \\ \text{s.t.} & (3) - (4), (7), (9) - (14) \\ & (15\mathbf{b}), (16), (18) - (23\mathbf{b}) \\ & (26), (41) \\ & G^{t}_{\mathbf{w},1} \leq J^{t}_{\mathbf{w}} \quad \forall \ t \in \mathcal{T} \\ & G^{t}_{\mathbf{p},1} \leq J^{t}_{\mathbf{p}} \quad \forall \ t \in \mathcal{T} \end{split} \tag{CCO}$$

where slack variables $J_{\rm w}^t$ and $J_{\rm p}^t$ are upper bounds on the flexibility costs. Since these variables are minimized, the optimal solution will be to set them equal to $G_{\rm w}^t$ and $G_{\rm p}^t$.

We solve this problem using the scenario approach for convex problems [40] for a number of reasons. First, the uncertainty impacts the constraints in complex ways and it is not clear how to analytically reformulate the constraints using known uncertainty distributions. Second, we are unlikely to know the uncertainty distributions in practice and the scenario approach does not require this information. Third, the scenario approach gives us a way to enforce the constraints jointly, rather than individually as is typical with approaches that rely on analytical formulation. A drawback of the scenario approach is that it requires a significant amount of data. Additionally, it is often very conservative in practice [46], leading to empirical violation probabilities much lower than the user-selected violation level ϵ and, subsequently, higher costs. Specifically, in the approach, the constraints are enforced for a large set of uncertainty realizations resulting in a large convex deterministic optimization problem. The number N of scenarios required for probabilistic reliability guarantees is

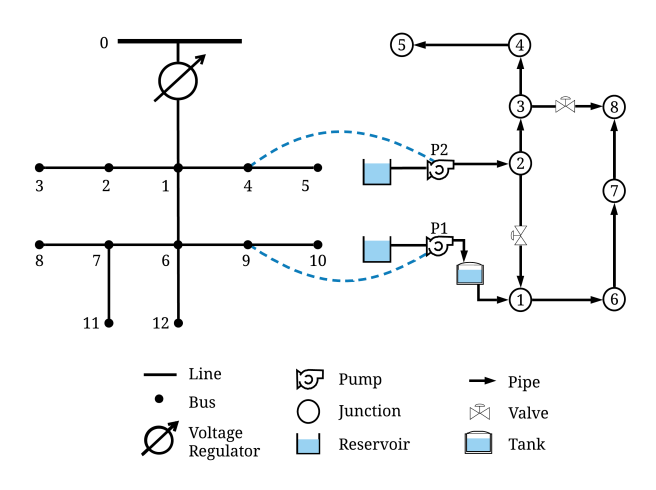


Fig. 3. Coupled PDN (left) and WDN (right). The dashed lines show where the water supply pumps are connected to the PDN. The water tank is passive. We show the single-phase equivalent PDN but we used a three-phase unbalanced network model. The pumps are modeled as balanced three-phase loads.

determined based on a user-selected violation level ϵ and confidence level ψ [40]

$$N \ge \frac{2}{\epsilon} \left(\ln \frac{1}{\psi} + \delta \right) \tag{42}$$

where δ is the number of decision variables in the optimization problem. In our case, the probabilistic guarantees apply to the convex (approximate and relaxed) problem, not the nonconvex problem. While there are some related approaches and results for nonconvex problems, they do not appear to apply directly to the form of our nonconvex problem. Further investigation of this issue is a subject for future research.

III. CASE STUDIES

In our case studies, we use the coupled WDN and PDN shown in Fig. 3, which we also used in [39]. We first describe the setup and then present and interpret the results. Additionally, we explore the impact of the convex relaxations on the WDN constraints, an approach to reduce the dimension of our power control policy parameters, and the choice of the flexibility cost formulation.

A. Setup

The WDN was originally presented in [16]; it is based on an actual WDN. We have modified it to include a cylindrical storage tank (25-m diameter, 30-m height, 30-m elevation), removed the booster pump, and converted the resistance coefficients from Hazen–Williams coefficients to Darcy–Weisbach coefficients. We changed the elevations at junction 6 and the reservoir upstream of pump 1 to 10 m and the minimum pressure heads at junctions 7 and 8 to 20 m. The pump hydraulic function coefficients are $m_{e=1}^0 = 75$ m and $m_{e=1}^1 = 0.005$ h/m² for pump 1 and

 $m_{e=2}^0=$ 90 m and $m_{e=2}^1=0.001$ h/m 2 for pump 2. We set $eta_\phi=2.322 imes10^{-3}$ kW/CMH \cdot m \forall ϕ \in Φ .

The unbalanced three-phase PDN uses the IEEE 13-bus feeder topology, where the real power load and line parameters are from [47]. We assume that all loads are wye-connected and constant power. Consumer loads have a 0.9 lagging power factor and pumps have a real-toreactive power ratio of 3 (i.e., a 0.949 lagging power factor). The distributed load between buses 1 and 6 is placed at bus 1. The minimum and maximum voltage limits are 0.95 and 1.05 pu. We set the voltage at the feeder head equal to 4.16 kV line-to-neutral. We assume the switch is closed and ignore the voltage regulator, shunt admittances, and the transformer between buses 4 and 5. Since we have no voltage regulator, we add capacitive loads (i.e., reactive power injections) to increase the system voltages: 100 kVAr at bus 8, phase c, and 200 kVAr at bus 10, all phases. For the base case power control policy, each pump has 17 control policy parameters corresponding to the number of buses and phases that have a load present.

We set the price of electricity to \$100/MWh for all pumps and time periods in the scheduling horizon. We set the flexibility cost weighting coefficients $g_{\rm w}^t$ and $g_{\rm p}^t$ to 1 or 1, where the latter is a row vector of ones and the units are selected to ensure that the flexibility costs are in \$ (specifically, the units of $g_{\rm w}^t$, $g_{\rm p}^t$ are [\$], [\$-kW²/CMH²] for Option 1; [\$/CMH] for Option 2; and [\$/kW] for Option 3). We conduct a sensitivity analysis to study the impact of varying $g_{\rm w}^t$ and $g_{\rm p}^t$ in Section III-E. Unless otherwise stated, we use flexibility cost Option 1 to generate our results; however, Section III-E compares all options. We set the chance constraint confidence level $\psi = 10^{-4}$ and vary ϵ .

To generate water and power demand forecast error scenarios, we draw samples from Gaussian probability distributions that are truncated at three standard deviations from the mean. For water demand forecast errors \tilde{d}_{i}^{t} , we use a mean of 0 and a standard deviation of $0.10\tilde{d}_{i}^{t}$. For power demand forecast errors, we use a mean of 0 and a standard deviation of $0.04\rho_{k,\phi}^t$. We do not model correlations in water and power demand forecast error, correlations across time, or correlations across space. While we would not expect actual forecast errors to be Gaussian and uncorrelated, these simplistic assumptions allow us to demonstrate how the approach works. Importantly, the approach works for forecast errors following any distribution and with any correlations; if sufficient amounts of real data were available, we could use it directly within our formulation.

We solve the problem with the JuMP package in Julia using the Gurobi solver [48]. We use a 64-bit Intel i7 dual core CPU at 3.40 GHz and 16-GB RAM.

To evaluate the reliability of our solutions, we use the Monte Carlo method to test whether all WDN and PDN constraints are satisfied for each of the 100 000 randomly generated uncertainty realizations. We draw these realizations from the same water and power demand forecast

Table 1 Case Studies

Case	Number of	Demand N	Required	
	Periods	Water	Power	Scenarios
A	1	1.00	1.50	4,369
В	3	[1.00,1.00,1.00]	[1.50,1.50,1.50]	13,107
C	3	[1.00,0.85,0.65]	[1.50,1.45,1.35]	13,107

error probability distributions as we used to generate the scenarios needed to reformulate the CC optimization problem. We use the realizations to compute the real-time control actions. The empirical violation probability is defined as the percentage of realizations for which at least one constraint is not satisfied.

B. Illustrative Results

We conduct three case studies described in Table 1. The water and power demand multipliers are used to modify the nominal water and power demands uniformly across all junctions in the WDN and all buses in the PDN. When expressed as a vector, each entry corresponds to one time period. We also report the number of forecast error scenarios required by the scenario approach when $\epsilon=5\%$.

Fig. 4 shows the pump/tank scheduled flow rates corresponding to the CC problem (CCO) presented in Section II-H versus the convex deterministic problem (D3) presented in Section II-E for Case B, $\epsilon=5\%$ (left) and Case C, $\epsilon=5\%$ (right). Case B has constant high water and power demand whereas Case C has decreasing water and power demand. The figure also shows the flow rate

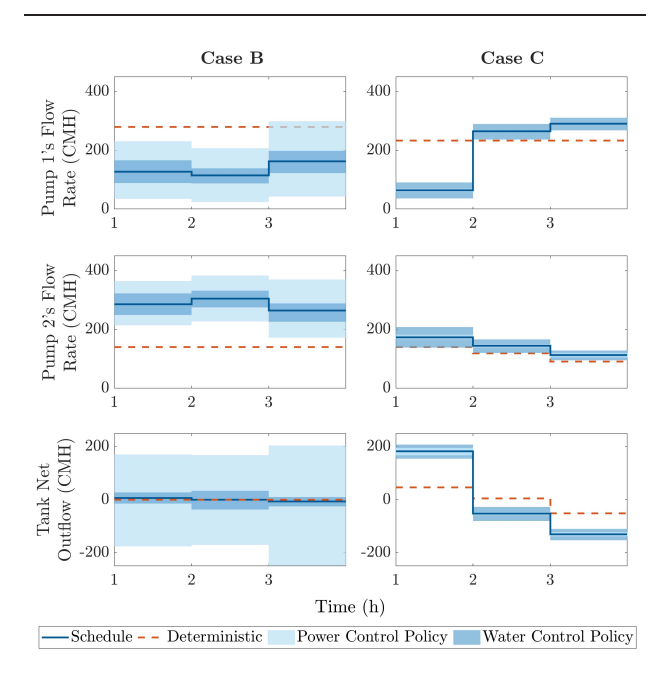


Fig. 4. Pump and tank schedules for Case B, $\epsilon=5\%$ (left) and Case C, $\epsilon=5\%$ (right). Dark and light blue shading show the flexibility bands around the scheduled flow rate associated with the water and power control policy, respectively. The schedule obtained from solving the deterministic problem is also shown.

flexibility bands associated with the water and power control policies, which can be calculated using (33) and (34), respectively. The flexibility bands are set to the largest pump flow adjustments and tank net outflow deviations obtained by applying the control policies to the forecast error scenarios used to solve (CCO). The empirical violation probabilities are 0.13% for Case B and 0.16% for Case C, both much smaller than ϵ .

We observe that the pump and tank schedules obtained from (CCO) vary more from period to period than those obtained from (D3). This is necessary to ensure that the forecast error scenarios do not lead to violations of the PDN constraints. Pump 1 is more efficient (and thus less expensive) than pump 2. However, pump 1 is located at bus 9, which is closer to its minimum voltage limit than bus 4 (where pump 2 is located). In order to satisfy the voltage constraints corresponding to the scenarios in Case B, pump 1's scheduled flow rate is lower than that obtained from solving the deterministic problem while pump 2's scheduled flow rate is higher than that obtained from solving the deterministic problem. This results in a more expensive operating point.

In Case C, pump 1's and the tank's schedules vary more from period to period than in Case B. Specifically, in Case C, when the power demand is highest (period 1), pumping is reduced and the tank is used to meet a significant portion of the water demand in order to satisfy the voltage constraints corresponding to the scenarios. Later, when demands are lower, extra pumping is used to refill the tank. In each period the system is operating far from the PDN constraints; in the first period, this is because of the reduction in pumping, and in subsequent periods, this is because of the reduction in water and power demand. Therefore, the power control policy parameters and associated flexibility bands are extremely small. In contrast, in Case B, there is less opportunity for pump load shifting and tank usage due to the high constant demands. Furthermore, the optimal schedule results in an operating point much closer to the PDN constraints, requiring much larger power control policy parameters and resulting in much larger flexibility bands. In both cases, we find that the flexibility bands associated with the water control policy remain approximately constant. This is expected since the water control policy is balancing water supply and demand.

Fig. 5 displays the pump flow rate adjustments from the schedule for Case A, $\epsilon=3\%$. They are obtained by applying the water control policy, power control policy, and both control policies to the 100 000 water and power demand forecast error realizations used to calculate the empirical violation probabilities. We differentiate between actions that: 1) satisfy WDN and PDN constraints; 2) satisfy WDN constraints but violate PDN constraints; 3) satisfy PDN constraints but violate WDN constraints; and 4) violate both WDN and PDN constraints. The overall empirical violation probability is 0.11%, which is much smaller than the ϵ we have selected. Of the set of realizations that

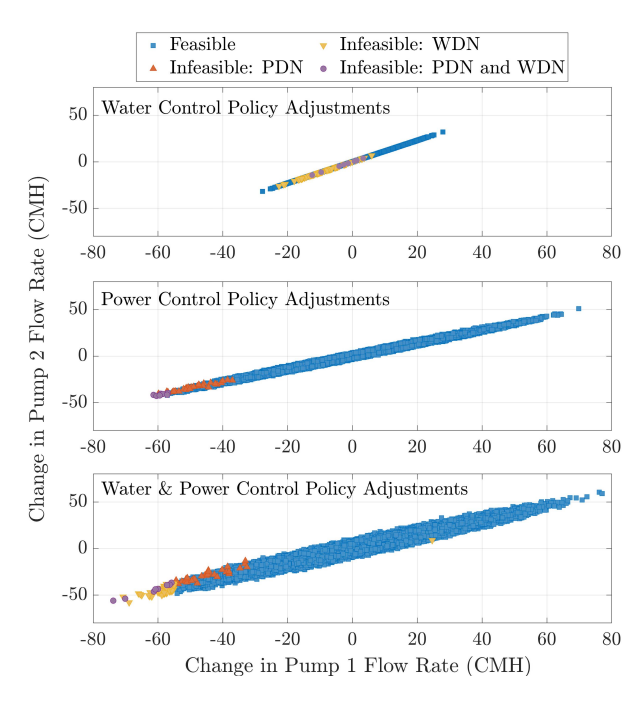


Fig. 5. Feasible and infeasible pump flow rate adjustments given water and power demand uncertainty for Case A, $\epsilon=3\%$.

violate any constraints, only 7.27% violate both WDN and PDN constraints. From the figure, we can also see that pump 1's adjustments are usually larger than pump 2's. This is because its power control policy parameters are larger (also visible in Fig. 4). Pump 1 has a more direct impact on PDN constraint satisfaction since it is located at bus 9, which is closer to its minimum voltage limit than bus 4 (where pump 2 is located). To visualize this, in Fig. 6, we plot the relative magnitude of each pump's negative power control policy parameters per bus and per phase on the PDN's three-phase voltage profile. The significant voltage unbalance is due to uneven, heavy loading. The power control policy generally contains both negative and positive parameters. Given an increase in power demand, a negative parameter reduces the pump's flow rate and

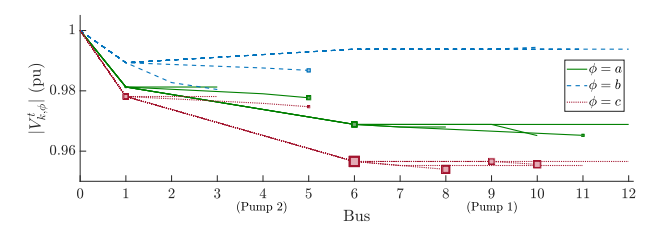


Fig. 6. Three-phase PDN voltage profile for the schedule in Case A, $\epsilon=3\%$. The square markers at each bus and phase are scaled according to the magnitude of the power control policy parameters. The dark squares represent pump 1's control policy parameters. The overlaying light squares correspond to pump 2's control policy parameters.

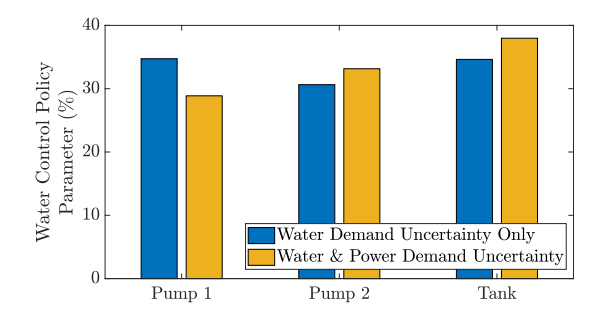


Fig. 7. Water control policy pump and tank contribution given: 1) only water demand uncertainty and 2) water and power demand uncertainty for Case A, $\epsilon=3\%$.

power consumption to respond to a minimum voltage limit violation, while a positive parameter increases the pump's flow rate to maintain the water supply. Therefore, by only showing the magnitude of the negative parameters, we can see the buses and phases where an increase in load is most likely to cause voltage limit violations, and which pump needs to reduce its power consumption more. We observe that pump 1's negative parameters always have a larger magnitude (and therefore a larger pump flow rate adjustment) than pump 2's negative parameters. Additionally, the control policy parameters associated with phase c are the largest since the voltages are close to the minimum voltage limit on phase c.

Next, we investigate how the water control policy parameters differ when we include only water demand uncertainty versus both water and power demand uncertainty. Fig. 7 shows the water control policy parameters for Case A, $\epsilon=3\%$. With only water demand uncertainty, pump 1's scheduled flow rate is higher than that of pump 2 and pump 1 contributes more to balancing water demand forecast error. However, with both water and power demand uncertainty, the solution becomes more conservative, that is, pump 1 reduces its flow rate and its contribution to water balancing. In our case studies, we find that power demand forecast error has a larger impact on the optimal schedules; however, it may have a larger or smaller impact than water demand forecast error on real-time pump adjustments, as shown in Fig. 4.

C. Impact of Convex Approximations and Relaxations

In this section, we first analyze the impact of: 1) the convex hull relaxation of the pipe head loss equation; 2) the approximate (linearized) pump hydraulic function; and 3) the convex hull relaxation of the pump power consumption curve. Considering only water demand uncertainty, we solve two variants of (CCO). The first one replaces the pipe head loss convex hull (21a) and (21b) with the original nonconvex head loss constraint (15c) where n=2. The second one replaces the linearized pump hydraulic function (22) with a quadratic one, where the quadratic

Table 2 Relaxation and Approximation Comparison

Formulation	Scheduled Flow Rate (CMH)			Head (m)							Tank Head (m)		
	Pump 1	Pump 2	1	2	3	4	5	6	7	8	Inlet	Outlet	
(CCO)	248.80	171.20	44.43	95.17	94.57	91.71	89.93	29.96	31.86	41.38	86.24	45.00	
Quadratic pipe head loss equation	248.80	171.20	44.48	95.17	94.64	92.88	92.24	31.77	33.07	41.72	86.24	45.00	
Quadratic pump hydraulic function	248.88	171.12	44.43	94.88	94.09	91.34	89.65	30.51	32.65	41.55	79.47	45.00	

coefficients for pumps 1 and 2 are -1.0941×10^{-4} and -1×10^{-5} h/m², respectively. We solve both variants with the scenario approach using the same number of scenarios as needed for the convex formulation. However, since neither variant is convex, the scenario approach solution no longer comes with probabilistic guarantees.

Table 2 shows the scheduled pump flow rates and the hydraulic heads for Case A, $\epsilon=5\%$ for (CCO) and both variants. (CCO) finds the same scheduled pump flow rates as the variant using the quadratic pipe head loss equation. However, the hydraulic heads obtained using the quadratic pipe head loss equation are all greater than or equal to the heads found in (CCO) since the actual head loss is the lower bound of the convex hull's feasible region, shown in Fig. 2. Since we are primarily concerned with minimum hydraulic head limits, use of the convex hull ensures that the solution does not violate those limits. While the hydraulic heads found using the convex hull of the pipe head loss are not exact, in our case studies we found that we can recover the exact hydraulic heads; however, this may not always be possible. Singh and Kekatos [49] prove uniqueness of the water flow equations for radial networks and certain meshed networks, for example, WDNs that have meshed network sections that do not contain pumps or valves, and meshed network sections with pumps that are not in cycles. They recovered the hydraulic heads by solving a convex energy minimization problem given the pump flow rates. While their proof does not extend to meshed networks containing pressure reducing valves, like ours, the solutions to our case studies appear unique and we are able to recover the heads corresponding to the quadratic pipe head loss equation in Table 2.

The linear pump hydraulic function overestimates the head gain and power consumption of the pumps. As a result, (CCO) overestimates hydraulic heads at junctions downstream of pumps. Components such as storage tanks and pressure reducing valves act as buffers, helping to correct the downstream hydraulic heads. For example, the outlet tank head is dependent on the tank water level; even if there is a difference in the inlet hydraulic head between (CCO) and the variant with the quadratic pump hydraulic function, the outlet head is identical for both formulations. We find that the formulations produce similar scheduled pump flow rates and slightly different hydraulic heads (Table 2). As expected, the inlet tank head obtained using the quadratic pump hydraulic function is lower than that obtained from (CCO). The outlet tank heads are identical. Additionally, the hydraulic heads for junctions 2-5 are smaller when we use the quadratic

Table 3 Empirical Violation Probabilities for Convex and Nonconvex Constraints

Case	ϵ	Proba	bility (%)	Voltage Violations (pu)			
	(%)	convex	nonconvex	minimum	average		
A	5	0.11	10.98	0.94717	0.94937		
	3	0.11	10.98	0.94717	0.94940		
В	5	0.12	35.16	0.94693	0.94935		
	3	0.10	34.29	0.94697	0.94937		
C	5	0.13	5.41	0.94732	0.94943		
	3	0.05	4.23	0.94724	0.94944		

pump hydraulic function since (CCO) overestimates pump 2's head gain.

The convex hull relaxation of the pump power consumption curve (23a) and (23b) does not impact the solution. This is because, when minimizing the WDN's electricity cost, the solution will lie on the lower bound of the convex hull, that is, the original constraint (17).

Lastly, we used the Monte Carlo method to evaluate the performance of the solutions of (CCO) within both the convexified network constraints and the original, nonconvex network constraints. Table 3 shows the empirical violation probabilities for each case and violation level. The nonconvex constraints are violated much more frequently than the convex constraints. All scenarios that violate the convex constraints also violate the nonconvex constraints. The additional violations of the nonconvex constraints are all voltage limit violations, indicating that the WDN approximations and relaxations are reasonable for this test system. We summarize the statistics of the additional voltage violations in the last two columns of the table, which show the minimum and average of the set of voltages below the minimum voltage limit corresponding to scenarios that violate the nonconvex constraints, but not the convex constraints. The minimum is just below the 0.95-pu minimum voltage limit indicating that the convex PDN model slightly overestimates the minimum voltages, as also shown in Fig. 8. We find that the difference between the actual voltage and the voltage calculated using the convex model (again, considering only the voltages that violate the nonconvex constraints, but not the convex constraints) is always less than or equal to 0.33%. Therefore, a simple way to cope with this issue would be to heuristically adjust the minimum voltage limit in the convex formulation to 0.955 pu. Alternatively, one could use a more accurate convex PDN power flow model, for example, one that includes loss approximations. For example, using the linearized, unbalanced three-phase power flow formulation with approximated losses from [43] instead of the lossless formulation from [44] on Case A, $\epsilon = 5\%$, and with the power demand multiplier reduced

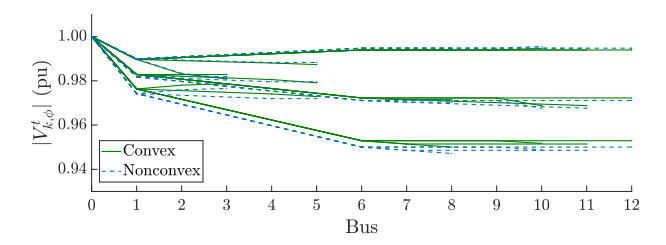


Fig. 8. Comparison of the three-phase PDN voltage profile corresponding to the approximate, convex power flow model and the original, nonconvex power flow model for a scenario in Case A, $\epsilon=5\%$.

from 1.500 to 1.465, we find that the empirical nonconvex violation probability decreases from 5.354% to 0.210%. Note that we reduced the multiplier because Case A was tuned to represent extreme conditions and so the problem was infeasible with the power flow formulation with approximated losses.

These observations call attention to the fact that our approach gives us no insights into or way to manage the magnitude or duration of constraint violations. This is a drawback of the type of chance constraint we are using. In our future work, we plan to explore alternative formulations that allow us to model and control constraint violations in a way that better matches the application-specific needs of the system, for example, allowing deviations but assigning a cost related to the magnitude of the deviation, or allowing deviations for limited time duration.

D. Simplifying the Power Control Policy

In this section, we investigate the impact of reducing the number of power control policy parameters to improve the computational tractability of our approach. The power control policy (27) uses a separate control policy parameter for each bus and phase with a load present, resulting in up to $3|\mathcal{K}|$ power control policy parameters. We refer to this as the base case. Here, we explore associating control policy parameters with groups of buses, for example, all buses on a lateral. To compute the control action, the control policy parameter is multiplied by the sum of power demand forecast errors in that group. With fewer control policy parameters, we need fewer scenarios since the number of scenarios is a function of the number of decision variables; this improves the computational tractability of the approach. Furthermore, this approach requires fewer measurements and a simpler communication systems, which would reduce the implementation costs. We consider two simplifications referred to as simplification 1 (S1) and simplification 2 (S2). Fig. 9 shows the groups of buses, referred to as zones, used for S1 and S2. We do not group phases. For example, in S2 there are two zones but six control policy parameters, one for each phase in each zone. We solve the base case and cases corresponding to both simplifications for Case A using flexibility cost Option 2 and considering only power demand uncertainty. We choose

flexibility cost Option 2 instead of Option 1 so that the flexibility costs are comparable across the cases. Flexibility cost Option 1 uses the Frobenius norm of the power control policy parameter matrix, which is a different size in each case, meaning the costs are not comparable across cases.

Table 4 shows the results including the number of power control policy parameters per pump and the number of scenarios for different values of ϵ . The table also reports the solver time, the energy cost associated with the schedule, the flexibility cost associated with the power demand control policy, and the empirical violation probability. As expected, the solver time generally decreases with fewer zones, meaning fewer decision variables and fewer scenarios. We expect the reduction in solver time would be more important in larger networks and/or for problems with longer scheduling horizons. Investigating other methods to improve the computational tractability of our approach is an area of future work.

In this case study, we find that S1 and S2 generally have lower empirical violation probabilities and higher objective costs than the base case. The base case has more degrees of freedom than S1 or S2, and so it is less conservative and lower cost. The control policy parameters associated with the simplifications cause coarser, larger, and more costly adjustments, which are more likely to be feasible against unseen scenarios. All cases have empirical violation probabilities much lower than ϵ , demonstrating that the scenario approach is conservative, which is typical [46]. Furthermore, all approaches produce the same schedule and energy costs. The base case has the lowest flexibility cost (i.e., it makes the smallest pump/tank adjustments to respond to power demand forecast errors) while satisfying the desired violation level ϵ , and therefore it exhibits the best cost/performance tradeoff.

E. Comparison of Flexibility Cost Formulations

In this section, we explore the advantages and disadvantages of the three flexibility cost formulations presented in

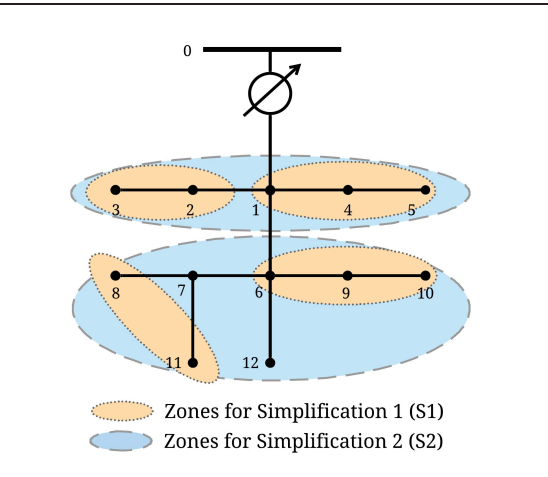


Fig. 9. Grouping of buses associated with power control policy parameters for simplification 1 (S1) and simplification 2 (S2).

Table 4 Power Control Policy Simplification Results

	Zones	Parameters per Pump	ε (%)	Scenarios	Solver Time (s)	Energy Cost (\$)	Flexibility Cost	Violation Probability (%)
Base Case	9	17	10	2,145	18.48	25.304	142.211	0.131
			5	4,289	29.95	25.304	145.581	0.116
			3	7,148	68.89	25.304	154.412	0.080
S1	4	9	10	1,825	7.49	25.304	155.925	0.135
			5	3,649	16.50	25.304	156.346	0.098
			3	6,081	29.83	25.304	158.751	0.056
S2	2	6	10	1,705	4.32	25.304	160.558	0.081
			5	3,409	14.47	25.304	162.684	0.066
			3	5,681	20.71	25.304	163.400	0.064

Table 5 Flexibility Cost Comparison

Option	Simplification	Solver Time (s)	Energy Cost (\$)	Scheduled Flow Rate (CMH)		Flexibility Cost		Violation Probability (%)
				Pump 1	Pump 2	Water	Power	
1	Base Case	38.04	25.64	77.55	342.34	0.34	1.19	0.109
	S1	17.95	24.82	160.01	259.99	0.33	1.24	0.044
2	Base Case	52.52	25.28	113.62	306.38	130.20	177.00	0.216
	S1	32.75	25.26	115.64	304.36	143.35	177.00	0.175
3	Base Case	252.28	25.31	110.95	309.06	0	76.54	0.117
	S1	73.29	25.31	110.95	309.06	0	82.32	0.096

Section II-G. We evaluate each flexibility cost formulation using Case A, $\epsilon=5\%$ and present the results in Table 5 for both the base case and simplification S1. We report the solver time, energy costs associated with the schedule, the scheduled flow rates, the flexibility costs associated with the water control policy and the power control policy, and the empirical violation probabilities, which are all much lower than ϵ .

Option 1 has the smallest solver time, but it is difficult to interpret the flexibility costs and determine the weighting coefficients $g_{\rm w}^t$ and $g_{\rm p}^t$ such that the flexibility costs can be fairly compared against the energy costs. Furthermore, as mentioned above, the flexibility costs are not comparable across simplifications. In Table 5, we observe that the water flexibility cost is approximately 1/3, which implies that the three pumps/tanks were used approximately equally to compensate water demand forecast error, which is a direct result of the flexibility cost formulation.

In Fig. 10, we show how the choice of water and power flexibility cost weighting coefficients impact the scheduled

energy cost, $G_{w,1}^t$, and $G_{p,1}^t$ for Case A, $\epsilon = 5\%$. Comparing the left and right plots, we see that as g_p^t increases, the scheduled energy cost increases and $G_{p,1}^t$ decreases. This tradeoff is intuitive: as power flexibility becomes more expensive relative to the scheduled energy cost, $G_{p,1}^t$ is reduced but the schedule becomes more expensive. The water flexibility cost weighting coefficient g_w^t has a negligible impact on the scheduled energy cost and $G_{p,1}^t$, and a small impact on $G_{\mathbf{w},1}^t$ in Option 1. There are several reasons for this. The first is that the magnitude of $G_{w,1}^t$ is small relative to the other costs in the objective function. The second is that the water flexibility cost has a limited range given the nature of the water control policy and Option 1. Since the water control policy splits the response between two pumps and one tank, the feasible range of $G_{\mathbf{w},1}^t$ is [(1/3),1], where $G_{\mathbf{w},1}^t=(1/3)$ when the split is equal. Changes in $G_{w,1}^t$ depend upon the magnitude of g_{w}^{t} relative to g_{p}^{t} , for example, $G_{w,1}^{t}$ is large when g_{p}^{t} is large relative to g_w^t . This sensitivity analysis highlights that the weighting coefficients would need to be tuned for the system of interest.

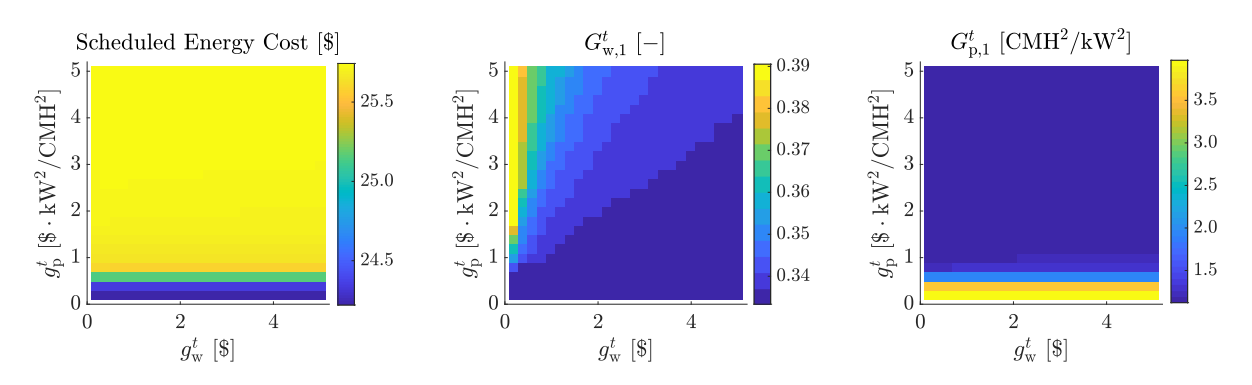


Fig. 10. Sensitivity analysis showing how the scheduled energy cost, $G_{w,1}^t$, and $G_{p,1}^t$ change when varying the weighting coefficients g_w^t [\$] and g_D^t [\$ · kW^2/CMH^2] for Case A, $\epsilon = 5\%$, and flexibility cost Option 1.

Option 2 provides more intuition on the flexibility costs, which are based on the largest pump flow rate adjustment required to address the scenarios needed for the scenario approach. For example, in Table 5, we can see that the power control policy produces larger maximum flow rate deviations than the water control policy, for both the base case and S1. Similar to Option 1, it is difficult to determine weighting coefficients that allows us to fairly compare flexibility costs to energy costs.

Option 3 uses the largest increase and decrease in pump power consumption from the scheduled consumption to define the flexibility costs. An advantage of this approach is that the flexibility cost and the energy cost are both a function of pump power consumption. However, there are two disadvantages to this approach. First, Option 3 has the largest solver time. Second, $R_{
m dn,p}^t$ and $R_{
m dn,w}^t$ will be inexact when using convex hulls, leading to a reduced downward flexibility band. Unlike the other flexibility cost options, Option 3 does not include tank flexibility costs since only pumps consume power. Therefore, the water control policy relies solely on the tank to balance water demand, and the water flexibility cost is 0, as shown in Table 5. By not including tank flexibility costs, there is no way to specify additional opportunity costs. However, tanks may be best equipped to respond to water demand forecast error since their purpose is to hedge against water demand variability [41].

Based on these results, it is not clear which flexibility cost option is best; however, Option 2 seems to exhibit good tradeoffs between tractability and interpretability. Also, in contrast to Option 3, it gives us a way to include the flexibility cost of the tanks.

IV. CONCLUSION

In this article, we formulated a CC water pumping problem subject to WDN and PDN constraints given water and power demand uncertainty. We developed power and water control policies that can be used in real time to respond to forecast errors. Control policy parameters are included as decision variables in the CC optimization problem. We reformulated the problem using convex approximations and relaxations and solved it with the scenario approach. Case studies explored solution patterns, which were found to be conservative (i.e., highly reliable at a high cost), in addition to the impact of the approximations and relaxations, an approach to simplify the power control policy, and the impact of different flexibility cost formulations.

We found that temporal and spatial shifting of WDN pumping load can be used support the PDN. We also found that convex approximations and relaxations used for the WDN were reasonable in that scenarios that violated the nonconvex constraints also violated the convexified constraints. However, the convex PDN model overestimated the smallest voltages leading to a large difference in the empirical violation probabilities corresponding to the convex constraints and the nonconvex constraints. Fortunately, this is easy to fix (heuristically) by slightly increasing the minimum voltage limit. Furthermore, we found that the approach is computationally heavy and does not currently scale to large networks or problems with long planning horizons. We proposed one way to simplify the power control policy, which reduces required measurements and also improves computational tractability, but results in more conservative solutions.

There are a number of remaining challenges that will be tackled in the future work. These include improving the computational tractability of the approach such that it could be applied to large networks and/or problems with long scheduling horizons; exploring alternatives to the scenario approach for solving the CC optimization problem; and developing approaches to minimize the need for large amounts of data, real-time measurements, and pervasive low-latency communication systems; developing formulations that cope with incomplete information about the PDN; and developing strategies for WDN/PDN information sharing and cooperation. Furthermore, we plan to explore the use of other convex power flow models, such as [43], which may improve the empirical violation probabilities corresponding to the original, nonconvex problem.

REFERENCES

- E. Dall'Anese, P. Mancarella, and A. Monti, "Unlocking flexibility: Integrated optimization and control of multienergy systems," *IEEE Power Energy Mag.*, vol. 15, no. 1, pp. 43–52, Jan. 2017.
- [2] A. Zlotnik, L. Roald, S. Backhaus, M. Chertkov, and G. Andersson, "Coordinated scheduling for interdependent electric power and natural gas infrastructures," *IEEE Trans. Power Syst.*, vol. 32, no. 1, pp. 600–610, Jan. 2017.
- [3] A. Shabanpour-Haghighi and A. R. Seifi, "An integrated steady-state operation assessment of electrical, natural gas, and district heating networks," *IEEE Trans. Power Syst.*, vol. 31, no. 5, pp. 3636–3647, Sep. 2016.
- [4] D. Olsen, A. Aghajanzadeh, and A. McKane, "Opportunities for automated demand response in California agricultural irrigation," Lawrence Berkeley Nat. Lab., Berkeley, CA, USA, Tech. Rep. LBNL-1003786, 2015.
- [5] I. Vijay, A. Aghajanzadeh, and O. Schetrit, "Low-cost, scalable, fast demand response for municipal wastewater and recycling facilities,"

- California Energy Commission, Sacramento, CA, USA, Tech. Rep. CEC-500-2015-086, 2015.
- [6] World Energy Outlook 2016, Int. Energy Agency, Paris, France, 2016.
- [7] D. Denig-Chakroff, "Reducing electricity used for water production: Questions state commissions should ask regulated utilities," Water Res. Policy, Nat. Regulatory Res. Inst., Columbus, OH, USA, Tech. Rep., 2008. [Online]. Available: https://pubs.naruc.org/pub/FA8644D5-C4EB-9E29-8D69-D75023FA0A9F
- [8] G. Klein, M. Krebs, V. Hall, T. O'Brien, and B. B. Blevins, "California's water-energy relationship—final staff report," California Energy Commission, Sacramento, CA, USA, Tech. Rep. CEC-700-2005-011-SF, 2005.
- [9] S. Pabi, A. Amarnath, R. Goldstein, and L. Reekie, "Electricity use and management in the municipal water supply and wastewater industries," Electr. Power Res. Inst., Palo Alto, CA, USA, Tech. Rep. 3002001433, 2013.
- [10] M. Chertkov and N. N. Novitsky, "Thermal

- transients in district heating systems," *Energy*, vol. 184, pp. 22–33, Oct. 2019.
- [11] M. Geidl and G. Andersson, "A modeling and optimization approach for multiple energy carrier power flow," in Proc. IEEE Russia Power Tech, Jun. 2005, pp. 1–7.
- [12] Z. Li, W. Wu, J. Wang, B. Zhang, and T. Zheng, "Transmission-constrained unit commitment considering combined electricity and district heating networks," *IEEE Trans. Sustain. Energy*, vol. 7, no. 2, pp. 480–492, Apr. 2016.
- [13] P. Mancarella, G. Andersson, J. A. Pecas-Lopes, and K. R. W. Bell, "Modelling of integrated multi-energy systems: Drivers, requirements, and opportunities," in Proc. Power Syst. Comput. Conf. (PSCC), Jun. 2016, pp. 1–22.
- [14] J. Söderman, "Optimisation of structure and operation of district cooling networks in urban regions," Appl. Thermal Eng., vol. 27, no. 16, pp. 2665–2676, Nov. 2007.
- [15] R. Salgado, E. Todini, and P. E. O'Connell, "Comparison of the gradient method with some

- traditional methods for the analysis of water supply distribution networks," in Computer Applications in Water Supply: Systems Analysis and Simulation, vol. 1. Taunton, U.K.: Research Studies Press Ltd., 1988, pp. 38-62.
- [16] D. Cohen, U. Shamir, and G. Sinai, "Optimal operation of multi-quality water supply systems—II: The Q-H model," Eng. Optim., vol. 32, no. 6, pp. 687-719, Jan. 2000.
- [17] P. W. Jowitt and G. Germanopoulos, "Optimal pump scheduling in water-supply networks," J. Water Resour. Planning Manage., vol. 118, no. 4, pp. 406-422, Jul. 1992.
- [18] J. E. van Zyl, D. A. Savic, and G. A. Walters, "Operational optimization of water distribution systems using a hybrid genetic algorithm," J. Water Resour. Planning Manage., vol. 130, no. 2, pp. 160-170, Mar. 2004.
- [19] B. Ghaddar, J. Naoum-Sawaya, A. Kishimoto, N. Taheri, and B. Eck, "A Lagrangian decomposition approach for the pump scheduling problem in water networks," Eur. J. Oper. Res., vol. 241, no. 2, pp. 490-501, Mar. 2015.
- [20] D. Fooladivanda and J. A. Taylor, "Energy-optimal pump scheduling and water flow," IEEE Trans. Control Netw. Syst., vol. 5, no. 3, pp. 1016-1026, Sep. 2018.
- [21] H. Mala-Jetmarova, N. Sultanova, and D. Savic, "Lost in optimisation of water distribution systems? A literature review of system operation," Environ. Model. Softw., vol. 93, pp. 209-254, Jul. 2017.
- [22] L. E. Ormsbee and K. E. Lansey, "Optimal control of water supply pumping systems," J. Water Resour. Planning Manage., vol. 120, no. 2, pp. 237-252, Mar. 1994.
- [23] A. P. Goryashko and A. S. Nemirovski, "Robust energy cost optimization of water distribution system with uncertain demand," Autom. Remote Control, vol. 75, no. 10, pp. 1754-1769, Oct. 2014.
- [24] I. Goulter, "Analytical and simulation models for reliability analysis in water distribution systems," in Improving Efficiency and Reliability in Water Distribution Systems, Dordrecht, The Netherlands: Springer, 1995, pp. 235-266.
- [25] P. Khatavkar and L. W. Mays, "Model for optimal operation of water distribution pumps with uncertain demand patterns," Water Resour. Manage., vol. 31, no. 12, pp. 3867-3880, Sep. 2017.
- [26] A. Babayan, Z. Kapelan, D. Savic, and G. Walters, "Least-cost design of water distribution networks under demand uncertainty," J. Water Resour.

- Planning Manage., vol. 131, no. 5, pp. 375-382, Sep. 2005.
- K. E. Lansey, N. Duan, L. W. Mays, and Y. Tung, "Water distribution system design under uncertainties," J. Water Resour. Planning Manage., vol. 115, no. 5, pp. 630-645, Sep. 1989.
- [28] D. Jung, D. Kang, J. H. Kim, and K. Lansey, "Robustness-based design of water distribution systems," J. Water Resour. Planning Manage., vol. 140, no. 11, Nov. 2014, Art. no. 04014033.
- [29] D. K. Molzahn and I. A. Hiskens, "A survey of relaxations and approximations of the power flow equations," Found. Trends Electr. Energy Syst., vol. 4, nos. 1-2, pp. 1-221, 2019.
- [30] E. DallAnese, K. Baker, and T. Summers, "Chance-constrained AC optimal power flow for distribution systems with renewables," IEEE Trans. Power Syst., vol. 32, no. 5, pp. 3427-3438, Sep. 2017.
- [31] L. Roald and G. Andersson, "Chance-constrained AC optimal power flow: Reformulations and efficient algorithms," IEEE Trans. Power Syst., vol. 33, no. 3, pp. 2906-2918, May 2018.
- [32] M. Vrakopoulou, B. Li, and J. L. Mathieu, "Chance constrained reserve scheduling using uncertain controllable loads. Part I: Formulation and scenario-based analysis," IEEE Trans. Smart Grid, vol. 10, no. 2, pp. 1608–1617, Mar. 2019.
- [33] L. Roald, S. Misra, T. Krause, and G. Andersson, "Corrective control to handle forecast uncertainty: A chance constrained optimal power flow," IEEE Trans. Power Syst., vol. 32, no. 2, pp. 1626-1637, Mar. 2017.
- [34] A. S. Zamzam, E. Dall'Anese, C. Zhao, J. A. Taylor, and N. D. Sidiropoulos, "Optimal water-power flow-problem: Formulation and distributed optimal solution," IEEE Trans. Control Netw. Syst., vol. 6, no. 1, pp. 37-47, Mar. 2019.
- [35] Q. Li, S. Yu, A. S. Al-Sumaiti, and K. Turitsyn, "Micro water-energy nexus: Optimal demand-side management and quasi-convex hull relaxation,' IEEE Trans. Control Netw. Syst., vol. 6, no. 4, pp. 1313-1322, Dec. 2019.
- [36] D. Fooladivanda, A. D. Dominguez-Garcia, and P. W. Sauer, "Utilization of water supply networks for harvesting renewable energy," IEEE Trans. Control Netw. Syst., vol. 6, no. 2, pp. 763-774, Jun. 2019.
- [37] K. Oikonomou and M. Parvania, "Optimal coordination of water distribution energy flexibility with power systems operation," IEEE Trans. Smart Grid, vol. 10, no. 1, pp. 1101–1110, Jan. 2019.

- [38] A. Stuhlmacher and J. L. Mathieu, "Chance-constrained water pumping to support the power distribution network," in Proc. North Amer. Power Symp., 2019, pp. 1-6, doi: 10.1109/NAPS46351.2019.9000282
- [39] A. Stuhlmacher and J. L. Mathieu, "Water distribution networks as flexible loads: A chance-constrained programming approach," in Proc. Power Syst. Comput. Conf., 2020, pp. 1-8.
- [40] M. C. Campi, S. Garatti, and M. Prandini, "The scenario approach for systems and control design," Annu. Rev. Control, vol. 33, no. 2, pp. 149-157, Dec. 2009.
- [41] D. Verleye and E.-H. Aghezzaf, "Optimising production and distribution operations in large water supply networks: A piecewise linear optimisation approach," Int. J. Prod. Res., vol. 51, nos. 23-24, pp. 7170-7189, Nov. 2013.
- [42] L. Gan and S. H. Low, "Convex relaxations and linear approximation for optimal power flow in multiphase radial networks," in Proc. Power Syst. Comput. Conf., Aug. 2014, pp. 1-9.
- [43] B. A. Robbins and A. D. Dominguez-Garcia, "Optimal reactive power dispatch for voltage regulation in unbalanced distribution systems." IEEE Trans. Power Syst., vol. 31, no. 4, pp. 2903-2913, Jul. 2016.
- [44] D. B. Arnold, M. Sankur, R. Dobbe, K. Brady, D. S. Callaway, and A. Von Meier, "Optimal dispatch of reactive power for voltage regulation and balancing in unbalanced distribution systems," in Proc. IEEE Power Energy Soc. Gen. Meeting, Jul. 2016, pp. 1-5.
- [45] P. R. Bhave and R. Gupta, Analysis of Water Distribution Networks. Oxford, U.K.: Alpha Science International, 2006.
- [46] M. Vrakopoulou, K. Margellos, J. Lygeros, and G. Andersson, "A probabilistic framework for reserve scheduling and N-1 security assessment of systems with high wind power penetration," IEEE Trans. Power Syst., vol. 28, no. 4, pp. 3885-3896, Nov. 2013.
- [47] W. H. Kersting, "Radial distribution test feeders," in Proc. IEEE Power Eng. Soc. Winter Meeting, vol. 2, Jan./Feb. 2001, pp. 908-912.
- [48] Gurobi Optimizer 8.1. Accessed: 2019. [Online]. Available: http://www.gurobi.com
- [49] M. K. Singh and V. Kekatos, "On the flow problem in water distribution networks: Uniqueness and solvers," 2019, arXiv:1901.03676. [Online]. Available: http://arxiv.org/abs/1901.03676

ABOUT THE AUTHORS

Anna Stuhlmacher (Student Member, IEEE) received the B.S. degree in electrical engineering from Boston University, Boston, MA, USA, in 2017, and the M.S. degree in electrical engineering from the University of Michigan, Ann Arbor, MI, USA, in 2019, where she is currently pursuing the Ph.D. degree.

Her research interest includes the optimization of uncertain distributed energy resources.



Johanna L. Mathieu (Senior Member, IEEE) received the B.S. degree in ocean engineering from the Massachusetts Institute of Technology, Cambridge, MA, USA, in 2004, and the M.S. and Ph.D. degrees in mechanical engineering from the University of California at Berkeley, Berkeley, CA, USA, in 2008 and 2012, respectively.



the Department of Electrical Engineering and Computer Science, University of Michigan, Ann Arbor, MI, USA. She was a Postdoctoral Researcher with the Swiss Federal Institute of Technology (ETH Zurich), Zürich, Switzerland. Her research interests include modeling, estimation, control, and optimization of distributed energy resources.